Metamaterial-Based Wearable Staircase Ultra-Wideband Antenna for Breast Cancer Imaging and WBAN Applications

Tale Saeidi[1*], Idris Ismail[1], Adam R.H. Alhawari[2], Sarmad Nozad Mahmood[3], Sameer Alani[4]

[1*]Electrical and Electronic Engineering Department of Universiti Teknologi PETRONAS, 32610 Bandar Seri Iskandar, Perak, Malaysia
[2]Electrical Engineering Department, College of Engineering, Najran University, Najran, Kingdom of Saudi Arabia
[3]Department of Electrical and Electronic Engineering, Faculty of Engineering, Universiti Putra Malaysia
[4]Centre for Advanced Computing Technology (C-ACT), Faculty of Information and Communication Technology, Universiti Teknikal Malaysia Melaka, Hang Tuah Jaya, 76100 Durian Tunggal, Melaka, Malaysia

Corresponding author* email: gs32772@gmail.com, talecommunication@gmail.com
Accepted Nov 2020, available online 30 December 2020

ABSTRACT

The proposed wearable antenna should have flexible, planar, and low-profile structure in order to fulfill the wearable antennas requirements applying for both wireless area body network and breast cancer imaging. The proposed wearable antenna consists of a layer of denim (11×11 mm^2) as substate and Shieldit conductive material. The antenna is combined with eighteen metamaterial (MTM) unit cells consuming an altered rectangular split ring resonator (SRR) to expand BW, increase the directive gain, and maintain the Specific Absorption Rate (SAR) value below 2 W/Kg. It works within a frequency range of 5.2-22.2 GHz and offers a maximum directive gain of 5.85 and radiation efficiency of more than 78%. The outcomes proved that only a little discrepancy exists between the simulated and measured results of the proposed antenna. Besides, it shows that the antenna elements can detect tumor with radius of 2 mm in a breast with maximum diameter of 320 mm. The results credibly demonstrated the ability of the proposed wearable UWB antenna system for both wireless body area network (WBAN) and breast cancer imaging applications.
Keywords: metamaterial, wearable antenna, miniaturized, WBAN, breast cancer imaging, UWB

1. Introduction

Several applications such as embedded smart systems, communications, and health monitoring purposes were benefited using wearable and flexible antennas have been produced for various applications. The current fast expansion of wearable wireless devices and WBAN has drew several researchers to get involve in the similar area of study. The current chaotic conditions in the hospitals and its standard operational procedures (S.O.P.) because of the COVID-19 pandemic challenges had forced the healthcare specialists aware about the necessity of growth in contactless medical procedures to shun the infection to spread rapidly. There should be an innovation to prevent the patients to contact with others, especially the staff nurse can carry out their vital checkup remotely [1, 2]. This could be a perfect way to publicize and ease the WBAN usage [3]. Most of the designed on-body devices having miniature dimensions, light, and sometimes robust. For instance, the stretchable antennas that can simply provide a consistent and high-performance communications [4]. Since the WBAN communication devices are worn on-body, they are vulnerable in bending condition or when they touch the skin directly. This may disintegrate the antennas' radiation characteristics and disturb the impedance matching. Besides, it reduces the system's radiation efficiency and received signals. The wearable devices might be crammed or fixed on body and so their performances affected by body movements. The body conditions such as temperature and sweating also alter the system's performances. Consequently, to face and resolve these challenges, this paper introduces a cost-effective miniaturized and flexible antenna which can be worn easily as compared to previous works [5-10]. These wearable antennas as a part of WBAN commutation system recommend higher solution and conformability in detection of patients remotely without any need of going to the hospital for checkup, especially during the COVID-19 pandemic when the social distance is required by SOP. As well as in the absence of the pandemic, to avoid mixing with other sick people.

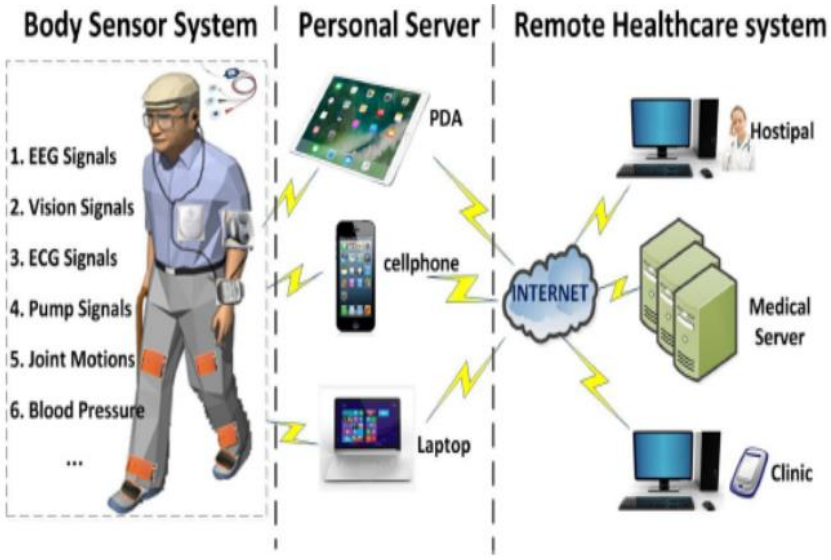

Figure. 1. A setup for health monitoring system [3]

An antenna is known as a vital component in a WBAN communication system [11]. Wearable antennas integration with different electronic components and systems needs more focus on decreasing the on-body conditions detuning on antennas performances. The antenna detuning effects depend on the antenna form-factor, its distance from the skin, and the body shape. These impacts can be suppressed by applying different structures improvements such as defected ground or truncated structures. Due to their flexibility and simplicity in integration, the antennas use flexible textile materials considered as good candidates for the WBAN communication systems [8]. Copious single, dual, and multiband flexible wearable antennas have been proposed offering excellent performance [12-29]; even when remote controlling in hospitals were important [30-33]. Besides, based on the consumption factor theory, the power efficiency improves with bandwidth (BW) and extra efficient energy is attainable when higher frequency band is used. Additionally, if an antenna demonstrates a high directive gain even with small physical dimensions, the attenuations can be suppressed. Although it can extend array integration using less printing area [34].

The wearable antennas should be designed carefully not to disturb the human body when they are worn. Therefore, the Specific Absorption Rate (SAR) should be considered during the designing procedure (should be less than 2. The meta surface, metamaterial integration with antenna, and can maintain the SAR value in the acceptable standard range. Numerous techniques applied to attain high directivity and gain using meta-surface, large intelligent surfaces (LIS) [35-37], at different frequency bands [38-39].

Several UWB antennas with capability of being worn were designed to operate at various bands such as 3.1-11.3 GHz [40], 2.9-11 GHz [41], 3-12 GHz [42], and 2.7-10.26 GHz [43]. For instance, a fractal patch mounted on a textile substrate to operate at 1.4-20 GHz for WBAN application [44] and for ISM applications [45]. A flexible planar quasi-Yagi UWB antenna designed for WBAN with the BW of 7.4 GHz and dimensions of 34×30 mm^2 [46]. In addition to those, more wearable UWB antennas devised for WBAN communication and breast cancer detection [47-49].

2. Antenna Design

Figure 2 and Table 1show the proposed antenna's prototype and its dimensions. An ordinary elliptical shape patch antenna was designed initially, and it was fed using a transmission line (TL). It designed on a denim substrate with ε_r= 1.2 and h= 0.67 mm. The initial dimensions of the antenna substrate are defined by applying the microstrip antenna equations presented in [50].

When the conventional antenna's outcomes attained, some stop-bands were seen over the working bandwidth of the antenna. Consequently, the examination of surface current distribution (SCD) is helpful at the working bands (Figure 3). Based on Figure 3 the SCD shows more density around the TL and the modified patch and it says both affect the lower-end and higher-end of the band. Thence, the GND was cut into staircase shapes to improve the antenna's BW and suppress the stop-bands around 8.5 GHz. Besides, it expanded the BW, up to 21 GHz. After that, an arrow shape slot was etched from the patch to eliminate the stop-band around 12 GHz. Likewise, two slots with the shape of rectangular were removed to suppress the unwanted notches further and enhance the S_{11} at 18 GHz.

Not all the designing parameters affect the BW dramatically. These parameters can be listed as dimensions of patch (a, b) , the width and length of TL (L_f, W_f), the arrow wings (L_2), and the staircase dimensions (L_6, L_7, L_{f8}). For instance, L_f and b shift the BW, a and W_f affect the input impedance BW. Also, $L_{6\text{-}f8}$ improve and expand the BW too. A metamaterial (MTM) structure was integrated to enhance the overall performance of the proposed antenna in terms of the BW, the radiation characteristics like gain and directivity.

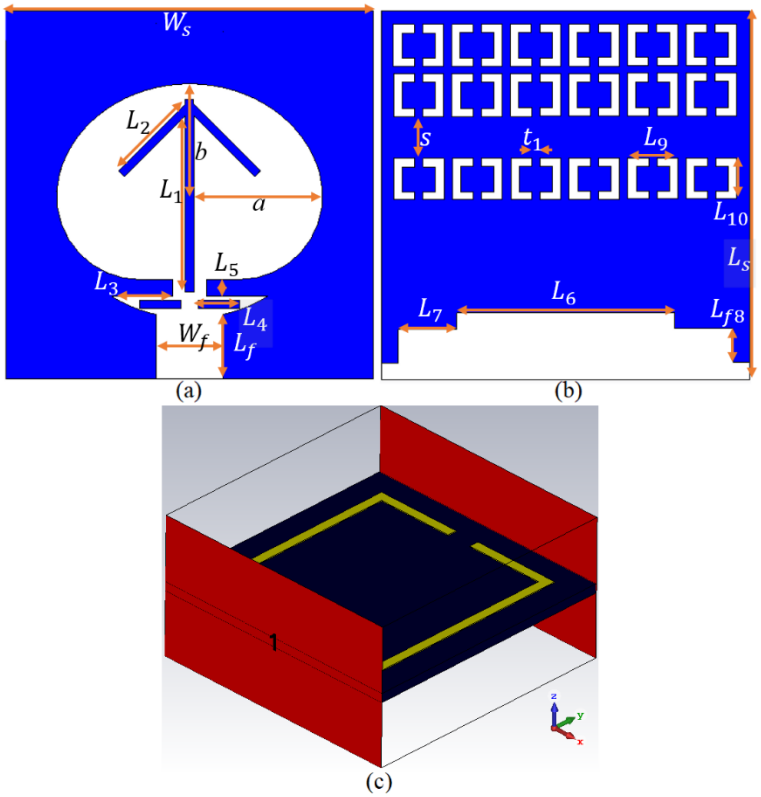

Figure. 2. The antenna's prototype: a) front view, b) back view, and (c) metamaterial single element

Table 1. Antenna dimensions

Parameters	Dimensions (mm)	Parameters	Dimensions (mm)
Ls	11	L_{f8}	1
L_f	2	L_9	1.5
L_1	5.28	L_{10}	1.25
L_2	2.83	W_s	11
L_3	1.83	W_f	2
L_4	1.25	a	4
L_5	0.5	b	3.5
L_6	6.5	s	1.25
L_7	1.75	t_1	0.25

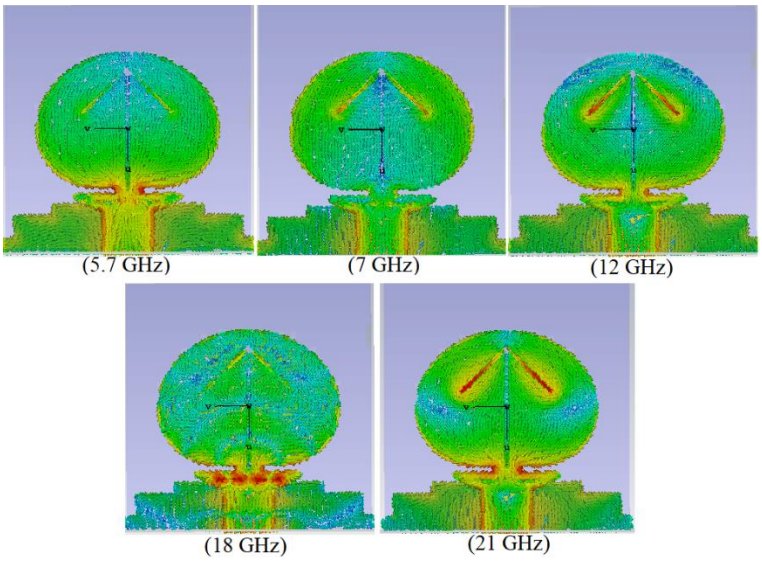

Figure. 3. The antenna's SCD without metamaterial arrays

The single element MTM structure consists of a modified rectangular shape SRR [51-52]. It magnetically resonates and produces the magnetic permeability by the perpendicular magnetic field [53-54]. It should be mentioned that any slits establish a capacitance which controls the structure's resonant specification. Also, the modified SRR was etched by a split to expand the SRR's series capacitance and lessen mutual coupling [51], [55]. Besides, the integration of the structures introduces a simultaneous electric (E) and magnetic (H) fields.

The MTM unit cell shown in Figure 1(c) was devised on a flexible textile 'denim' substrate with a ε_r and h of 1.2 and 0.7 mm, respectively. The finite integration technique (FIT) was used in CST Microwave studio to assess and the reflection and transmission coefficients of the antenna. To do so, magnetic/electric boundaries and two waveguide ports set around the MTM structure as both x-axis and y-axis considered as perfect magnetic and electric conductors, respectively. Likewise, an open space assumed towards the z-axis considered same as the MTM feeding. The MTM structure should be devised in a way to offer a negative index where the antenna is not operating. Plus, Nicolson-Ross-Weir (NRW) method reported in [56] was performed to examine the proposed MTM unit cell's electromagnetic (EMT) specifications. I EMT used to analyze and get the ε, μ, and n utilizing the simulated S_{11} and S_{21} as presented Figure 4 and 5. The operating BW range of ε, μ, n is summarized in Table 2. The S_{21} result indicates a peak around 17.5 GHz. The antenna is integrated with the MTM arrays to enhance the antenna's radiation characteristics like impedance matching, radiation efficiency, etc.

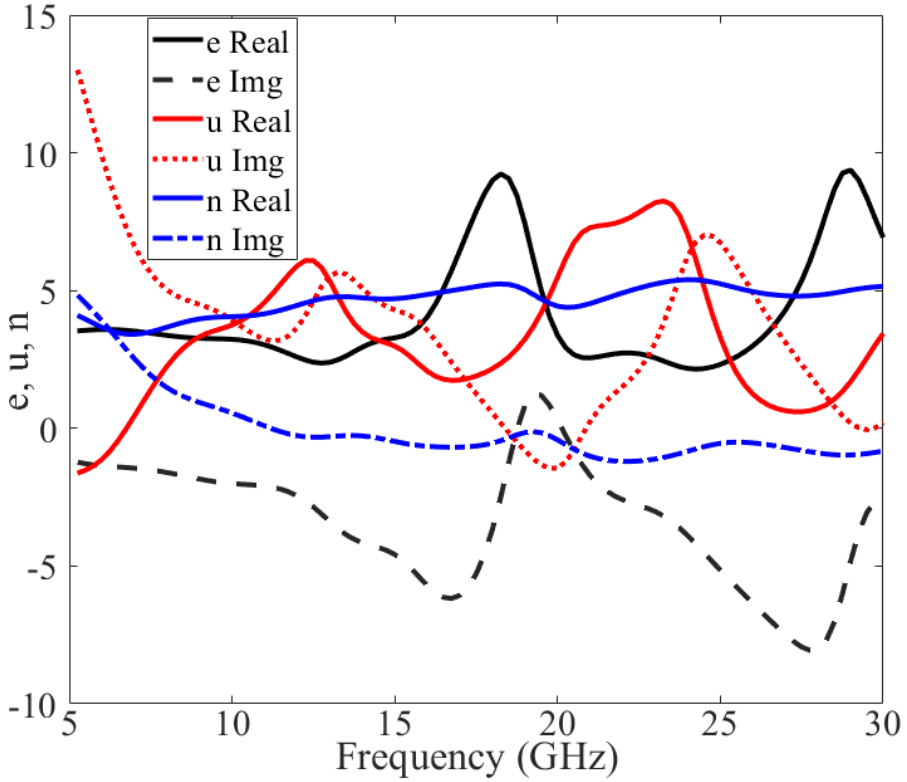

Figure. 4. The retrieved effective parameters of the MTM unit cell

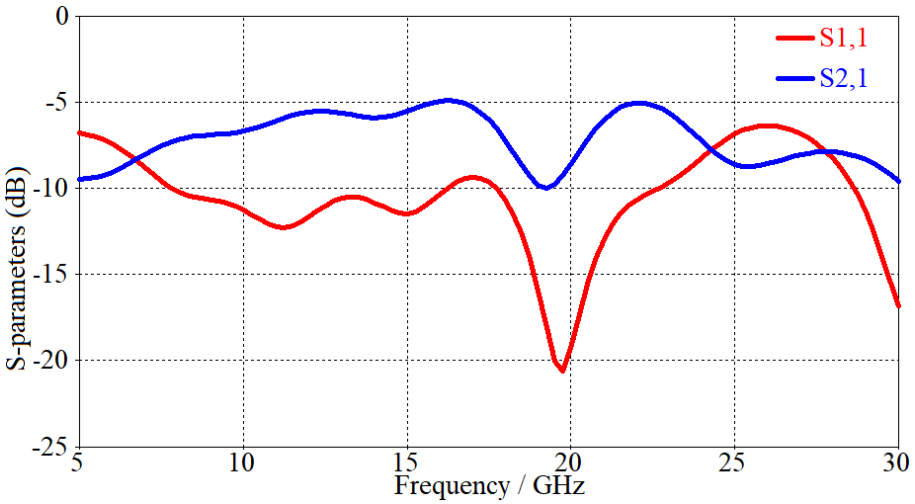

Figure. 5. S-parameter results of single MTM structure

Table 2. Negative index frequency regions of the MTM unit cell

Factors	(ε)	(μ)	(n)
Functional BW (GHz)	5-18, 22-30	17-22	11-30

3. Results and Discussion

The antenna performance should be evaluated for both conditions of on and off-body, with and without MTM structures applying the simulation setup presented in Figure 6. In the simulation setup, a woman body voxel is used for the imaging environment.

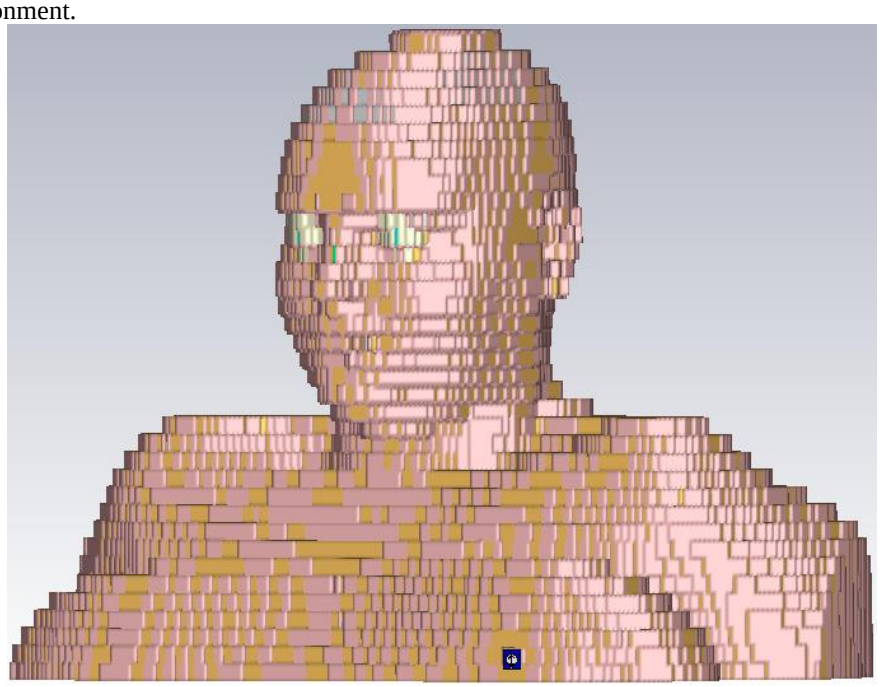

Figure. 6. The simulation setup of the imaging environment

When eighteen elements of MTM were used and incorporated with the antenna, improved outcomes were achieved as revealed in Figure 7. Interestingly, the performance of the antenna had enhanced more when the third row of MTM arrays were separated by *S* distance. Additionally, the reflection coefficient results were analyzed and compared when incorporated with and without MTM elements as presented in Figure 7. Essentially, the analysis was preceded by an investigation on the impacts of the element numbers on the performance of the antenna. The reflection coefficient results shown in Figure 6 present an improvement after adding the MTM elements for both on and off-body conditions.

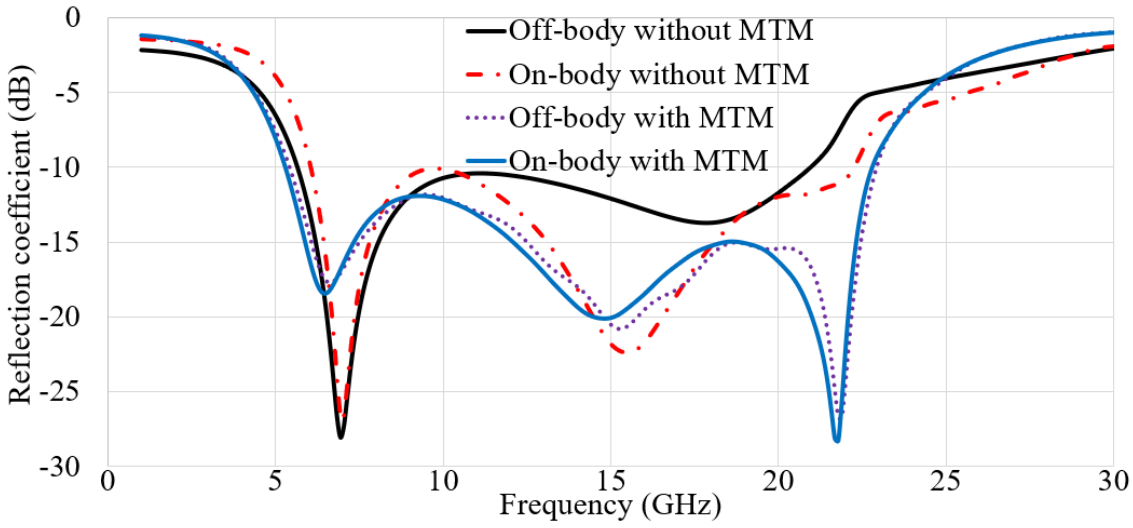

Figure. 7. Reflection coefficient results with and without MTM for both on and off-body conditions

As the results revealed in Figure 8, a narrower – 3 dB beam and significant enhancement in the directivity is obtainable only when the antenna is integrated with the MTM arrays.

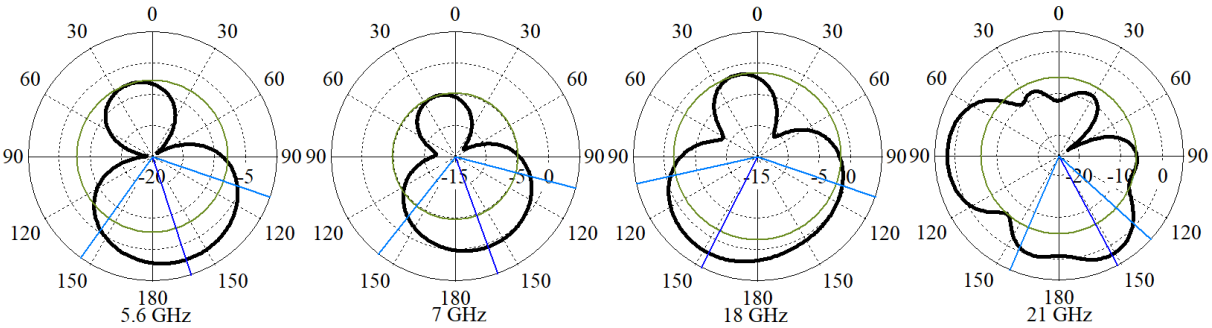

Figure. 8. The on-body radiation pattern of the antenna integrated with MTM structure

The gain of the antenna has been greatly improved by the MTM arrays about 2.5 dBi within its operating frequency band compared to the one without MTM structure. Similarly, the radiation efficiency has been enhanced about 10 % after incorporation with the MTM elements. Overall, it offers a outmost gain and radiation efficiency of 5.85 dBi and 94 % at the frequency of 18 GHz, respectively. Besides, the result shows that the radiation efficiency is higher than 78 % from 7 GHz to 23 GHz. Table 3 represents the performance of the proposed antenna compared with recent similar works in terms of gain, bandwidth, and dimensions. Favorably, as it is observable from Table 3, the proposed antenna has smaller size and high gain within its frequency bandwidth compared to the other antennas presented in Table 3. The results verified the capability of the proposed technique applied in this work to improve the overall performance of its antenna to suit both WBAN and breast imaging applications.

Table 3. Antenna performance comparison

Reference	Dimensions (mm^2)	BW (GHz)	Max Gain (dBi)
[57]	20 × 20	2 - 18	> -2.65
[58]	28.6 × 28.6	2 - 27	-
[59]	16 × 16	26 - 40	7.44
[60]	50 × 40	2.2 – 25	4.5
[61]	26 × 16	18 - 44	1.45
[62]	50.8 × 62	1.3 - 20	10
Proposed	11 × 11	5.1-23.5	5.85

Figure 9 depicts both simulated and measured S_{11} results of the antenna with MTM arrays on-body conditions are shown in. Finally, the simulated and measured results empirically yielded good agreement. All the operating poles were attained in the measurement. However, the band shifted slightly when it contacts the arm and the breast. Nonetheless, the S_{11} level was lessened by -5 dB roughly in comparison with the simulation outcomes. Besides, the reflection coefficient results on the chest were shifted down more than on the arm. Reasonwise, it might be due to different composition of the skin layers and structures whereby the skin maybe is thicker around the chest as compared to the arm [63-64].

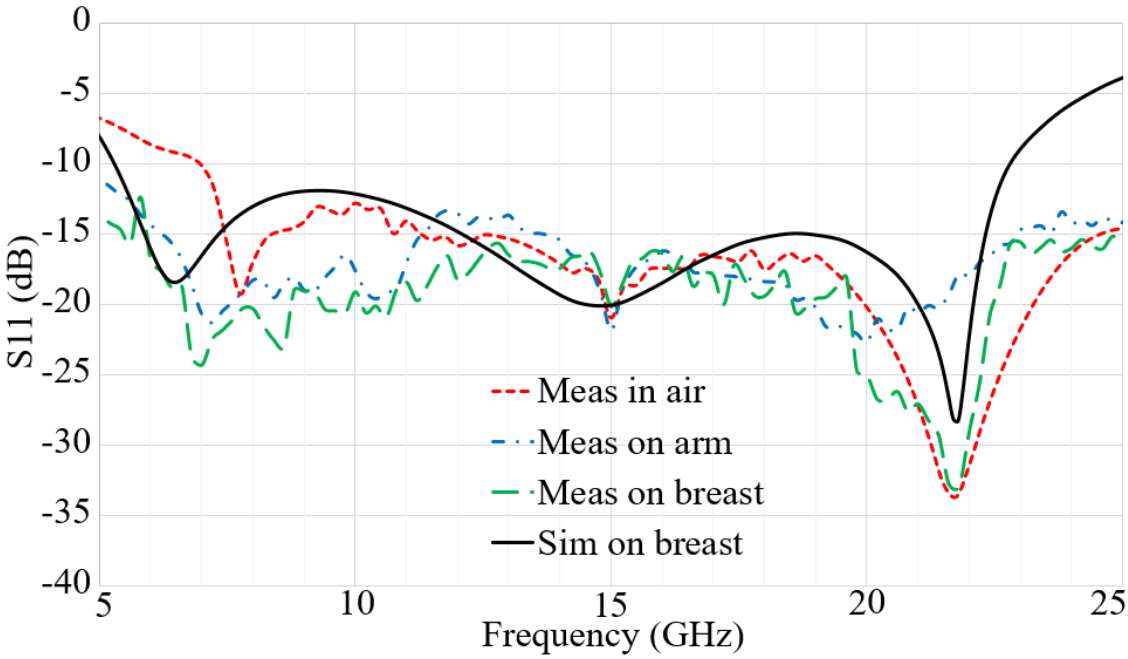

Figure. 9. Simulation and measurement in air, on breast, and arm

Another important factor that should considered for flexible wearable antennas is the SAR value. Based on the principles, it should be less than 2 W/Kg for both standards of 1g and 10g. Figure 10 and Table 4 present the result of SAR values on the layers of skin, breast fat, muscle, and bone at the working BW of the proposed antenna. The results showed that the SAR values met the standard requirements mentioned.

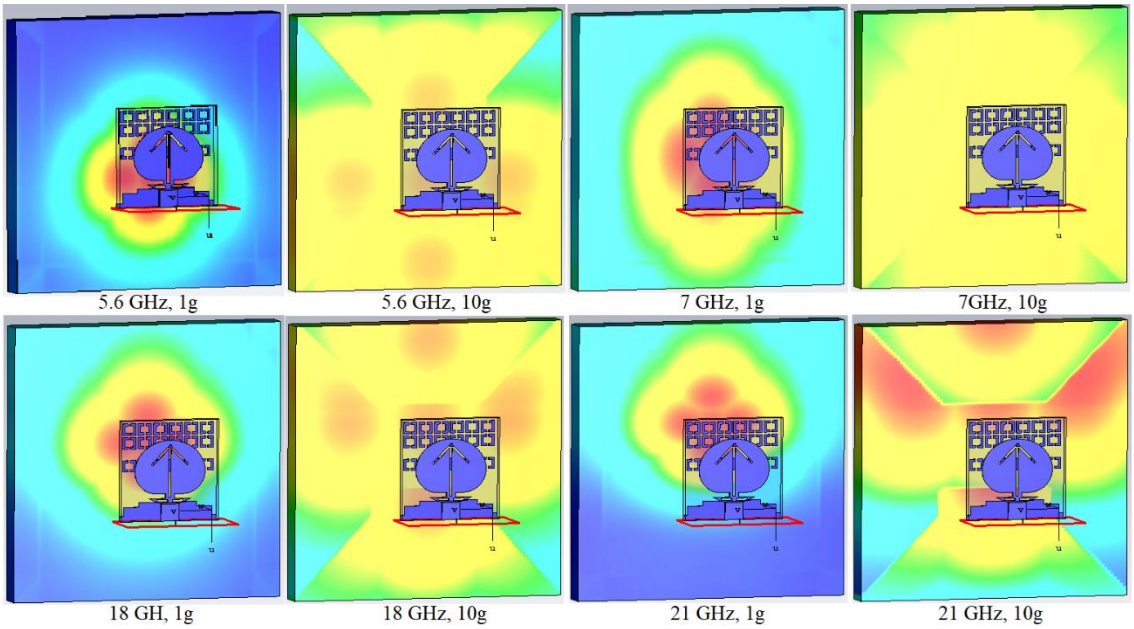

Figure. 10. SAR variation on body for both 1 g and 10 g at different frequencies

Table 4. SAR values at different frequencies

Frequency (GHz)	1 g	10 g
5.6	0.497	0.29
7	0.911	0.698
18	1.995	1.16
21	2.011	1.02

3.1 Investigations in the breast media

It would be informative to assess the antenna characteristics in both time (TD) and frequency domain (FD). Unlike the wide-band and UWB antennas, the narrow-bands are usually depicted in the FD. Likewise, the radiation characteristics and properties are considered constant over few percentages of the BW. A UWB structure is usually recognized in an impulse-based formation. Hence, the TD impacts and characteristics should be noticed and assessed. The FD system is presumed that uses a transmitter antenna which is triggered with a continuous wave. On the other hand, the TD description is excited using an impulse signal. The transient response of an antenna mostly alters on time, along with the departures and arrivals angles and polarization. The process of transmitting and receiving a pulse between every two UWB antennas in TD is depicted in Figure 11.

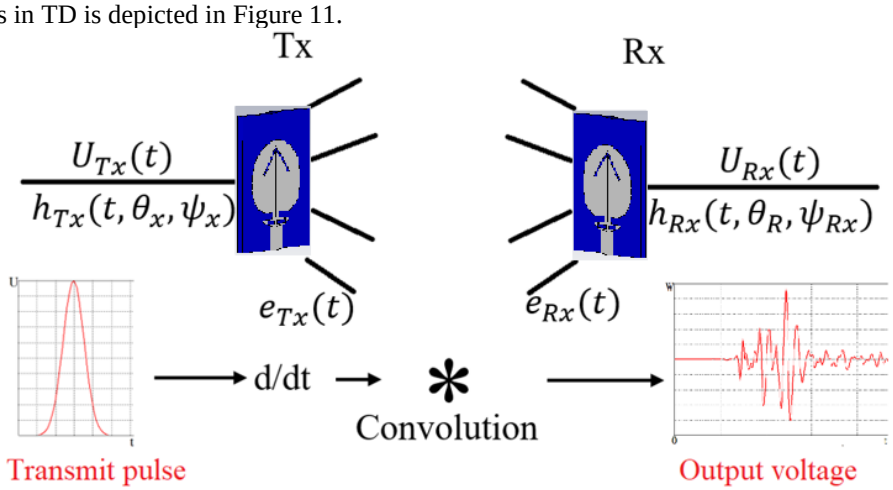

Figure. 11. Sending and receiving process of two UWB antennas

Before starting the construction an image of a tumor in the breast using the simulation data, several significant factors that should be examined. Figure 12 shows the simulation setup of the antenna array elements around the breast media and the tumor within it. The received signals should be considered first due to its important role in image reconstruction of the tumor. Array one (A1) is assumed as transmitter and the other array elements are considered as receivers. Based on what presented in Figure 13, the received signals' shape did not change dramatically but the signal's amplitude altered and shifted slightly.

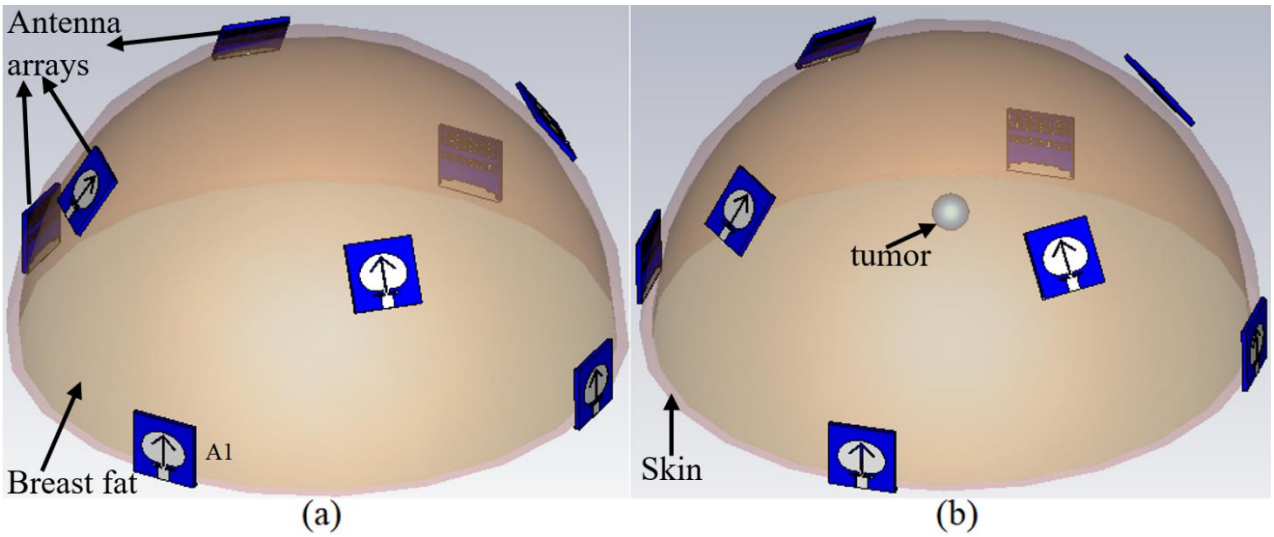

Figure. 12. The simulation setup of the breast model and the antenna elements

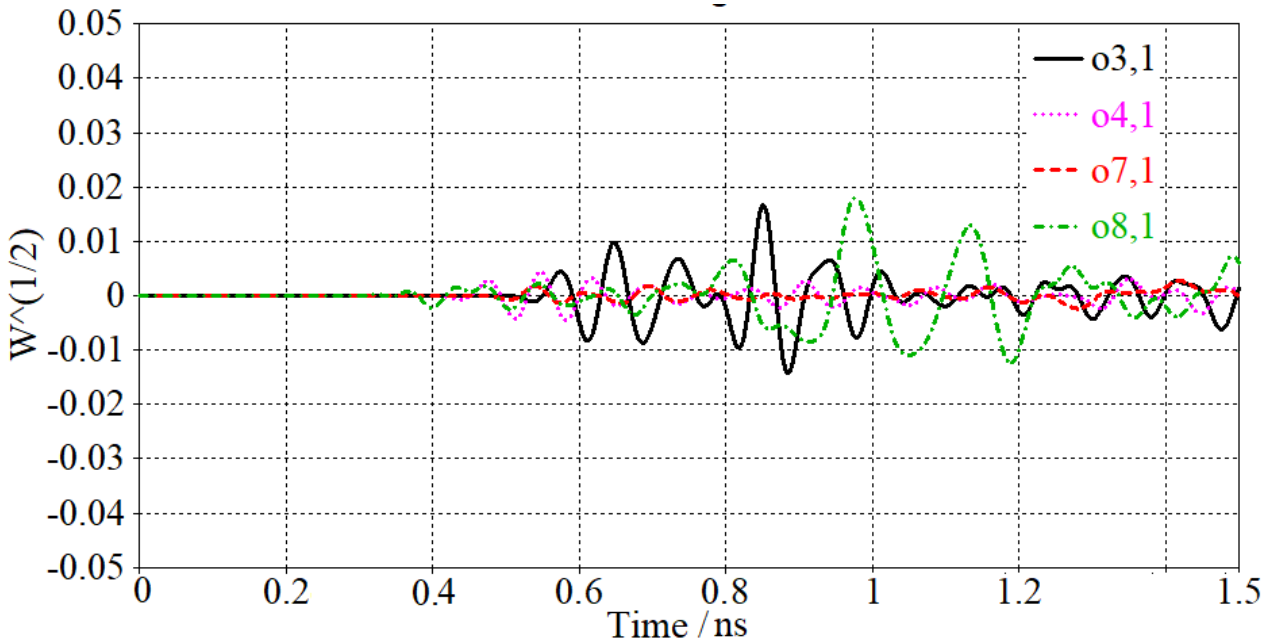

Figure. 13. The recipient signals from different arrays of the antenna on the breast model

A1 sends a UWB pulse and other antenna elements receive it. The received signals shown in Figure. 13 received from four array elements (A3, A4, A7, and A8) at the presence of tumor and they were shifted due to the delay and distance between every two array elements. They were located differently to demonstrate how distance and angle change the signal reception (Figure 12). Thus, signals have the same shape but with changes in amplitude that are specific for each array position. The fidelity factor (FF) is to depict the signals similarity and distortion level in signals [65]. The result in Figure. 14 illustrate that similarity of more than 90% achieved using both simulation and measurement data.

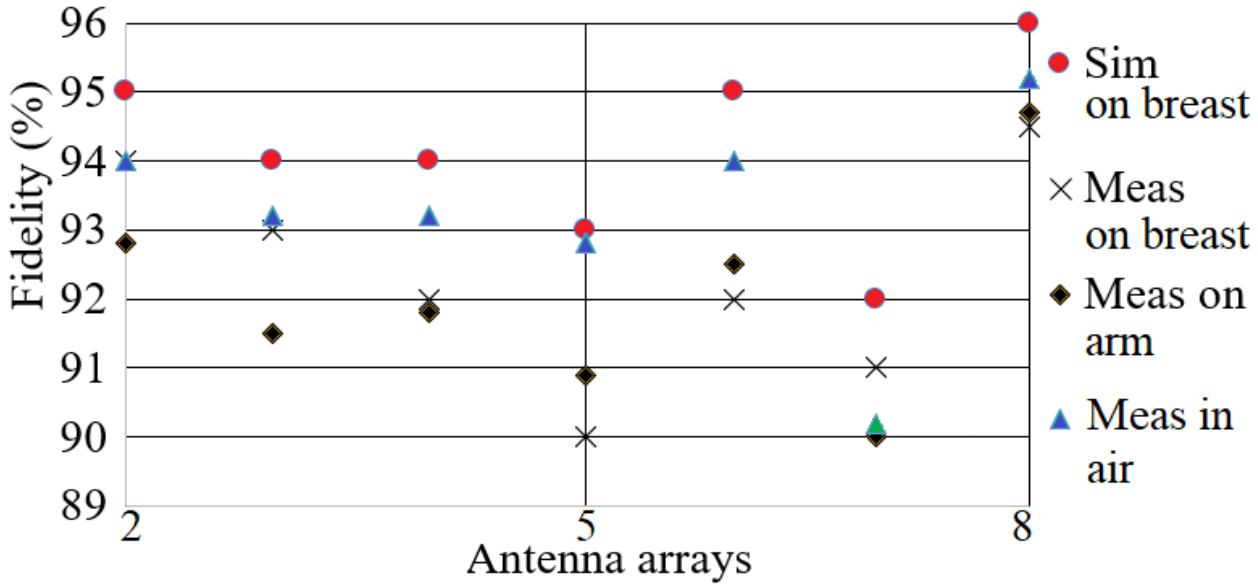

Figure. 14. Fidelity factor for simulation and measurement

The mutual coupling between every antenna array element is another essential parameter to be considered in imaging. Figure 15 shows how the mutual coupling and isolation factor are around the breast media and he tumor. Since the transmission coefficient level of the antenna array elements showing a level of less than– 15 dB at most of its working BW. It can be concluded that a very decent mutual coupling and isolation exist among the antenna arrays.

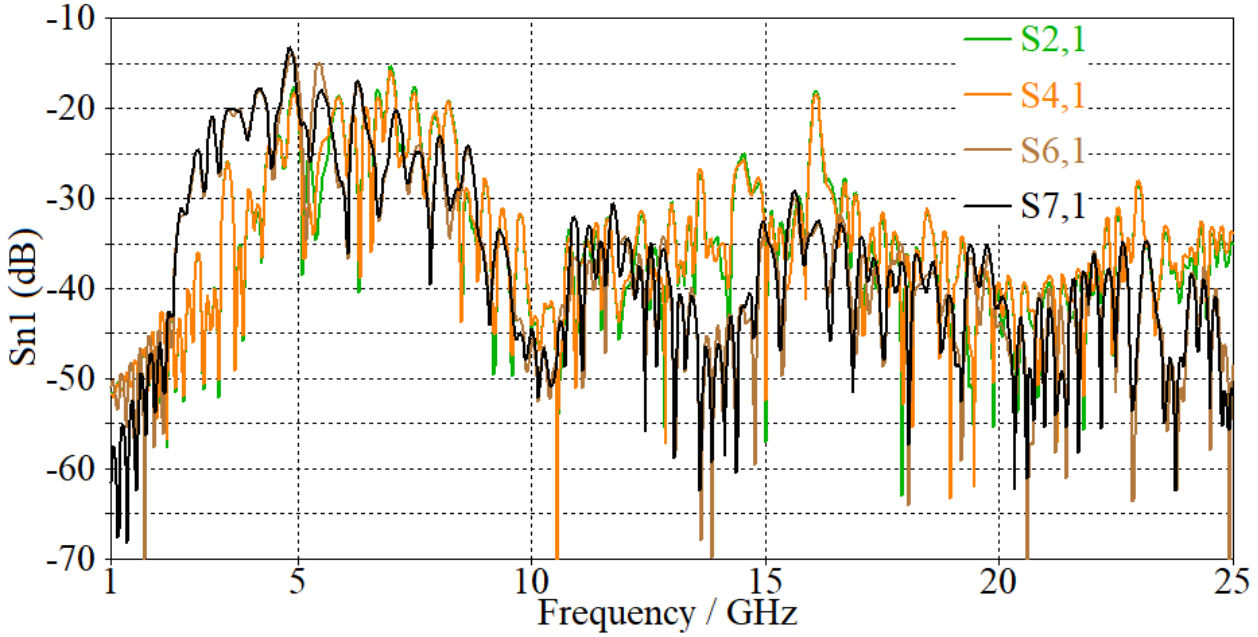

Figure. 15. The transmission coefficient results from four arrays of on-body

3.2 Image reconstruction tumor in breast

All the received signals presented in Figure 13 are obtained from CST and then imported to MATLAB to reconstruct the image of the tumor with a 2 mm radius by applying the simulation output data. The robust time-reversal (RTR) algorithm presented in [66] was used to recreate the image utilizing three assumptions such as number of arrays around a target (tumor), two off-centered tumors, and a breast sample with larger diameter. Figure 16 signifies the reconstructed image the central tumor using different number of array elements as three, five, and eight (the breast and tumor have the radius of 60 mm and 2 mm, respectively). The results offer a correct detection and localization of the tumor with radius of 2mm and a range resolution an approximate 6.5 mm based on the operating BW of the antenna as 17 GHz [67-69]. Therefore, a 2 mm radius tumor was selected for investigation to confirm whether the antenna elements are capable of detecting a tumor smaller than that dimensions. In addition, the images are the clearest when eight antenna array elements are used. It shows that the unwanted effected of the clutters produced by other array elements and the skin layer are completely suppressed.

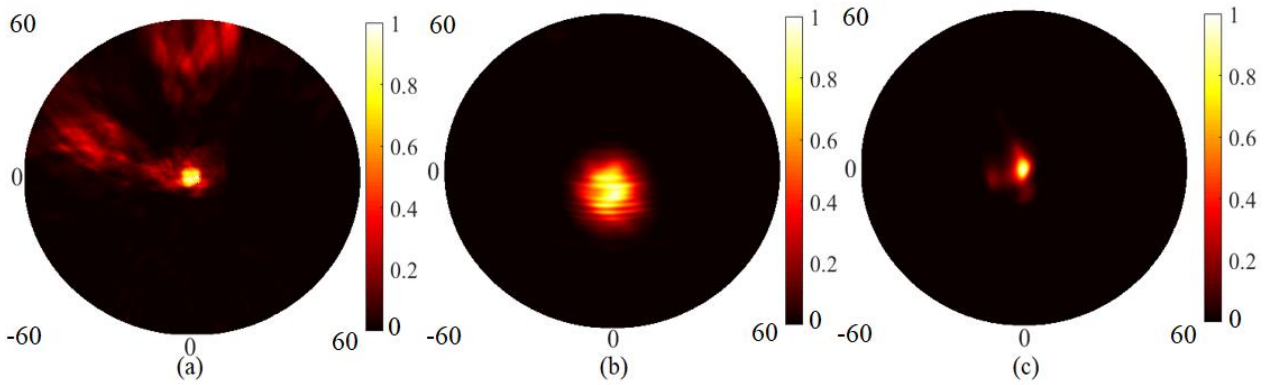

Figure. 16. The image of detected tumor utilizing RTR algorithm and different number of array elements (a) three, (b) five, and (c) eight array elements

One central and one off-center tumor are considered in breast with the same diameter to assess the antennas ability further. The RTR algorithm is applied again to detect the tumor through image reconstruction. Figure 17 shows both the central and the off-center tumors are detected properly with some insignificant clutters around the tumor.

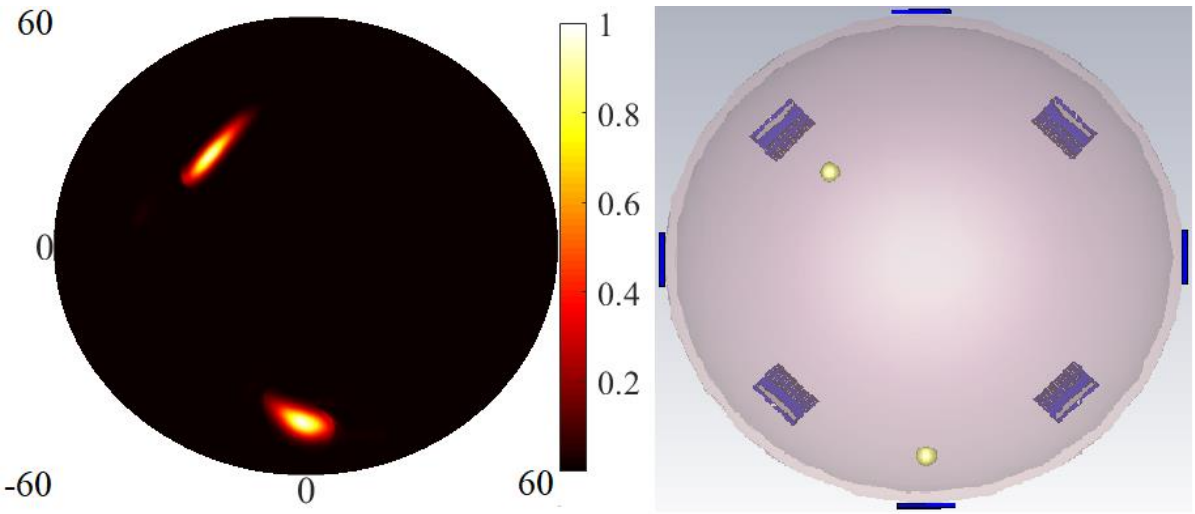

Figure. 17. Two tumors detected within the breast

Apart from considering more than two targets in breast, assuming a larger breast with diameter of 320 mm is also can help to evaluate the system capabilities in detection of tumor (2 mm radius). Figure 18 indicates that the antenna elements in the system detect and reconstruct the tumor even considering a larger breast media in simulation process.

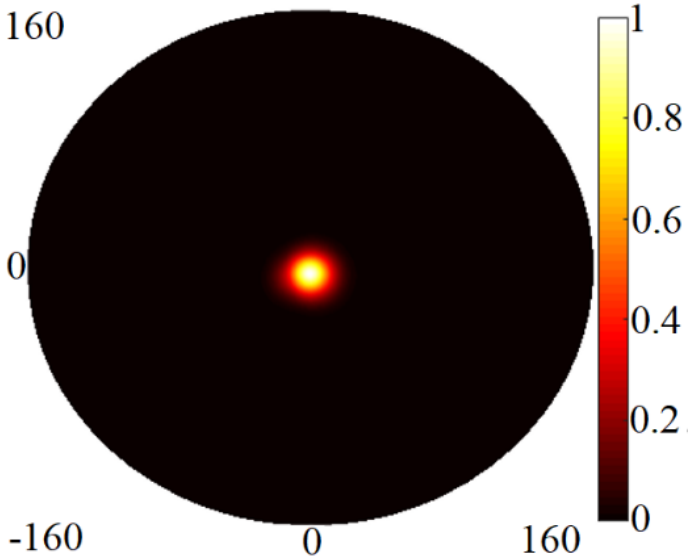

Figure. 18. Detected tumor within a larger breast with diameter of 320 mm

4. Conclusion

A metamaterial-based wearable staircase UWB antenna is integrated with eighteen MTM arrays for breast cancer imaging and WBAN applications. The MTM single cell comprises a modified SRR. Thence, the refraction index, permeability, and permittivity were computed for the single unit cell of MTM structure. After optimization of all the effective parameters of antenna, the improvement of antenna's performance in terms of gain, directivity, and BW were presented. The results show that less discrepancy exists between the simulated and measured results in different environments such as breast, arm, and free space with acceptable value of SAR (less than 2 W/Kg for both standards of 1 g and 10 g). The antenna obtained more than 78% radiation efficiency and maximum directional gain of 5.85 dB over at the operating frequency band. The proposed antenna elements system depicts an ability to sense a tumor with a radius of 2 mm inside the breast in different considerations such as two tumors and breast with larger size. Finally, the proposed wearable UWB antenna is a suitable economical candidate for both applications of WBAN and breast cancer imaging.

Acknowledgment

The authors appreciate University Technology PETRONAS for support of the project.

5. References

[1] "https://www.cdc.gov/coronavirus/2019-ncov/hcp/telehealth.html.".
[2] W. Wang, X. W. Xuan, P. Pan, Y. J. Hua, H. B. Zhao, and K. Li, "A low-profile dual-band omnidirectional Alford antenna for wearable WBAN applications," Microw. Opt. Technol. Lett., vol. 62, no. 5, pp. 2040–2046, 2020.
[3] http://english.sia.cas.cn/rh/rp/201812/t20181225_202798.html.
[4] T. W. Koo, Y. J. Hong, G. K. Park, K. Shin, and J. G. Yook, "Extremely low-profile antenna for attachable bio-sensors," IEEE Trans. Antennas Propag., vol. 63, no. 4, pp. 1537–1545, 2015.
[5] Q. H. Abbasi, A. Sani, A. Alomainy, and Y. Hao, "Arm movements effect on ultra wideband on-body propagation channels and radio systems," Loughbrgh. Antennas Propag. Conf. LAPC 2009 - Conf. Proc., pp. 261–264, 2009.
[6] Q. H. Abbasi, M. M. Khan, S. Liaqat, M. Kamran, A. Alomainy, and Y. Hao, "Experimental investigation of ultra wide-band diversity techniques for on-body radio communications," Prog. Electromagn. Res. C, vol. 34, pp. 165–181, 2012.
[7] Q. H. Abbasi, H. El Sallabi, N. Chopra, K. Yang, K. A. Qaraqe, and A. Alomainy, "Terahertz Channel Characterization Inside the Human Skin for Nano-Scale Body-Centric Networks," IEEE Trans. Terahertz Sci. Technol., vol. 6, no. 3, pp. 427–434, 2016.
[8] K. N. Paracha, S. K. Abdul Rahim, P. J. Soh, and M. Khalily, "Wearable Antennas: A Review of Materials, Structures, and Innovative Features for Autonomous Communication and Sensing," IEEE Access, vol. 7, pp. 56694–56712, 2019.
[9] Q. H. Abbasi, M. Ur Rehman, K. Qaraqe, and A. Alomainy, "Advances in body-centric wireless communication: Applications and state-of-the-art," Adv. Body-Centric Wirel. Commun. Appl. State-of-the-Art, pp. 1–438, 2016.
[10] M. M. Khan, Q. H. Abbasi, A. Alomainy, Y. Hao, and C. Parini, "Experimental characterisation of ultra-wideband off-body radio channels considering antenna effects," IET Microwaves, Antennas Propag., vol. 7, no. 5, pp. 370–380, 2013.
[11] M. N. Sudha and S. J. Benitta, "Design of antenna in Wireless Body Area Network (WBAN) for biotelemetry applications," Intell. Decis. Technol., vol. 10, no. 4, pp. 365–371, 2016.
[12] D. Mandal and S. S. Pattnaik, "Quad-band wearable slot antenna with low SAR values for 1.8 GHz DCS, 2.4 GHz WLAN and 3.6/5.5GHz WiMAX Applications," Prog. Electromagn. Res. B, vol. 81, pp. 163–182, 2018.
[13] M. Ur-Rehman, N. A. Malik, X. Yang, Q. H. Abbasi, Z. Zhang, and N. Zhao, "A Low Profile Antenna for Millimeter-Wave Body-Centric Applications," IEEE Trans. Antennas Propag., vol. 65, no. 12, pp. 6329–6337, 2017.
[14] A. Alemaryeen and S. Noghanian, "Crumpling effects and specific absorption rates of flexible AMC integrated antennas," IET Microwaves, Antennas Propag., vol. 12, no. 4, pp. 627–635, 2018.
[15] A. Alomainy, R. Di Bari, Q. H. Abbasi, and Y. Chen, "Antenna Design Requirements for Wireless BAN and WSNs," Co-op. Energy Effic. Body Area Wirel. Sens. Networks Healthc. Appl., pp. 7–23, 2014.
[16] P. J. Soh et al., "A smart wearable textile array system for biomedical telemetry applications," IEEE Trans. Microw. Theory Tech., vol. 61, no. 5, pp. 2253–2261, 2013.
[17] R. Yahya, M. R. Kamarudin, and N. Seman, "Effect of rainwater and seawater on the permittivity of denim jean substrate and performance of UWB eye-shaped antenna," IEEE Antennas Wirel. Propag. Lett., vol. 13, pp. 806–809, 2014.

[18] D. L. Paul, H. Giddens, M. G. Paterson, G. S. Hilton, and J. P. McGeehan, "Impact of body and clothing on a wearable textile dual band antenna at digital television and wireless communications bands," IEEE Trans. Antennas Propag., vol. 61, no. 4, pp. 2188–2194, 2013.
[19] Q. Bai and R. Langley, "Wearable EBG antenna bending and crumpling," in Loughborough Antennas and Propagation Conference, LAPC 2009 - Conference Proceedings, 2009, pp. 201–204.
[20] A. Y. I. Ashyap et al., "Compact and Low-Profile Textile EBG-Based Antenna for Wearable Medical Applications," IEEE Antennas Wirel. Propag. Lett., vol. 16, pp. 2550–2553, 2017.
[21] S. Yan and G. A. E. Vandenbosch, "Radiation Pattern-Reconfigurable Wearable Antenna Based on Metamaterial Structure," IEEE Antennas Wirel. Propag. Lett., vol. 15, pp. 1715–1718, 2016.
[22] E. F. Sundarsingh, S. Velan, M. Kanagasabai, A. K. Sarma, C. Raviteja, and M. G. N. Alsath, "Polygon-shaped slotted dual-band antenna for wearable applications," IEEE Antennas Wirel. Propag. Lett., vol. 13, pp. 611–614, 2014.
[23] R. B. V. B. Simorangkir, Y. Yang, L. Matekovits, and K. P. Esselle, "Dual-Band Dual-Mode Textile Antenna on PDMS Substrate for Body-Centric Communications," IEEE Antennas Wirel. Propag. Lett., vol. 16, pp. 677–680, 2017.
[24] J. G. Andrews, S. Buzzi, W. Choi, S. V. Hanly, A. Lozano, A. C. K. Soong, and J. C. Zhang, "What will 5G be?," IEEE Journal on Selected in Areas Communications, vol. 32, pp. 1065–1082, Jun. 2014.
[25] Faisal Tariq, Muhammad R. A. Khandaker, Kai-Kit Wong, Muhammad Imran, Mehdi Bennis, "A Speculative Study on 6G", IEEE Magezine, Feb 2019.
[26] S. V. Hum, and J. Perruisseau-Carrier, "Reconfigurable reflectarrays and array lenses for dynamic antenna beam control: A review," IEEE Transactions on Antennas Propagation, vol. 62, pp. 183-198, Jan. 2014.
[27] C. Borda-Fortuny, K.-F. Tong, A. Al-Armaghany, and K.-K. Wong, "A low-cost fluid switch for frequency-reconfigurable Vivaldi antenna," IEEE Antennas Wireless Propagation Letters, vol. 16, pp. 3151-3154, Nov. 2017.
[28] S. Chinchali et al., "Network Offloading Policies for Cloud Robotics: a Learning-based Approach," arXiv preprint arXiv:1902.05703, Feb. 2019.
[29] M. Chen et al., "Cognitive internet of vehicles," Computer Communications, vol. 120, pp. 58–70, May 2018.
[30] X.-F. Teng, Y.-T. Zhang, C. C. Poon, and P. Bonato, "Wearable medical systems for p-health," IEEE reviews in Biomedical engineering, vol. 1, pp. 62–74, Dec. 2008.
[31] M. J. W. Rodwell, Y. Fang, J. Rode, J. Wu, B. Markman, S. T. uran Brunelli, J. Klamkin, and M. Urteaga, "100-340GHz Systems: Transistors and Applications," in 2018 IEEE International Electron Devices Meeting (IEDM), Dec. 2018, pp. 14.3.1–14.3.4.
[32] M. Aladsani, A. Alkhateeb, and G. C. Trichopoulos, "Leveraging mmWave Imaging and Communications for Simultaneous Localization and Mapping," in International Conference on Acoustics, Speech, and Signal Processing (ICASSP), May 2019, pp. 1–4.
[33] T. S. Rappaport, "6G and Beyond: Terahertz Communications and Sensing," 2019 Brooklyn 5G Summit Keynote, Apr. 2019.
[34] Prem Chand Jain, "Wireless Body Area Network for Medical Healthcare", IETE Technical Review, Vol. 28, no.4, 2011.
[35] L. Zheng, J. Yang, H. Cai, W. Zhang, J. Wang, and Y. Yu, "MAgent: A many-agent reinforcement learning platform for artificial collective intelligence," in Proc. The 32nd AAAI Conference on Artificial Inteligence. AI (AAAI-18), 2018.
[36] Niamat Hussain and Ikmo Park, "Design of a wide-gain-bandwidth metasurface antenna at terahertz frequency", AIP Advances, April 2017.
[37] Sarawuth Chaimool, Tanan Hongnara, Chawalit Rakluea, Prayoot Akkaraekthalin, and Yan Zhao," Design of a PIN Diode-Based Reconfigurable Metasurface Antenna for Beam Switching Applications", International Journal of Antennas and Propagation, Volume 2019, 7 pages, 2019.
[38] Parul Dawar, N. S. Raghava, and Asok De, "UWB Metamaterial-Loaded Antenna for C-Band Applications", International Journal of Antennas and Propagation, Volume 2019, 13 pages, 2019.
[39] Jack Eichenberger, Ersin Yetisir, and Nima Ghalichechian, "High gain Antipodal UWB Vivaldi Antenna with Pseudoelement and Notched Tapered slot operating at 2.5-57 GHz", IEEE TRANSACTIONS ON ANTENNAS AND PROPAGATION, Vol. 67, no. 7, JULY 2019.
[40] Mariam El Gharbi,Marc Martinez-Estrada,Raul Fernández-García,Saida Ahyoud &Ignacio Gil, "A novel ultra-wide band wearable antenna under different bending conditions for electronic-textile applications", The Journal of The Textile Institute, May 2020.
[41] Srinivas Doddipalli, Ashwin Kothari, and Paritosh Peshwe, "A Low Profile Ultrawide Band Monopole Antenna for Wearable Applications", International Journal of Antennas and Propagation, Vol. 2017.
[42] Mohsen Koohestani, Nuno Pires, Anja K. Skrivervik, and Antonio A. Moreira, "Bandwidth Enhancement of a Wearable UWB Antenna Near a Human Arm", Microwave and Technology Letters, Vol. 55, no. 12, December 2013.

[43] Chow‐Yen‐Desmond Sim Chih‐Wei Tseng Hoang‐Jyh Leu, "Embroidered wearable antenna for ultrawideband applications", Microwave and Technology Letters, Vol. 54, no. 11, November 2012.
[44] M. Karimyian-Mohammadabadi,M.A. Dorostkar,F. Shokuohi,M. Shanbeh &A. Torkan, "Super-wideband textile fractal antenna for wireless body area networks", Journal of Electromagnetic Waves and Applications, Vol. 29, no. 13, 2015.
[45] Abirami AnbalaganORCID Icon,Esther Florence Sundarsingh,Vimal Samsingh Ramalingam,Aadesh Samdaria,David Ben Gurion &Karthik Balamurugan, "Realization and Analysis of a Novel Low-Profile Embroidered Textile Antenna for Real-time Pulse Monitoring", IETE Journal of Research, 17 July 2020.
[46] Veeraselvam Aruna,Mohammed Gulam Nabi AlsathORCID Icon,Savarimuthu Kirubaveni &Marimuthu Maheswari, "Flexible and Beam Steerable Planar UWB Quasi-Yagi Antenna for WBAN", IETE Journal of Research, 28 Nov 2019.
[47] Pranita Manish Potey &Kushal Tuckley, "Design of wearable textile antenna for low back radiation", Journal of Electromagnetic Waves and Applications, Vol. 34, no. 2, 2020.
[48] H. A. Shaban,M. A. El-Nasr &R. M. Buehrer, "Localization with Sub-Millimeter Accuracy for UWB-Based Wearable Human Movement", Journal of Electromagnetic Waves and Applications, Vol.25, no. 11-12, 2011.
[49] Praveen Kumar Rao and Rajan Mishra, "Elliptical Shape Flexible MIMO Antenna with High Isolation for Breast Cancer Detection Application", IETE Journal of Research, 23 Sep 2020.
[50] Ramesh Garg, Prakash Bhartia, Inder Bahl, and Apisak Ittipiboon, "Microstrip Antenna Design Handbook", ARTECH HOUSE, INC.
[51] M.M. Islam, M.T. Islam, M. Samsuzzaman and M.R.I. Faruque, "Compact metamaterial antenna for UWB applications", ELECTRONICS LETTERS, 6th August 2015 Vol. 51 No. 16 pp. 1222–1224.
[52] Marco Faenzi, Gabriele Minatti, David González-Ovejero, Francesco Caminita, Enrica Martini, Cristian Della Giovampaola & Stefano Maci, "Metasurface Antennas: New Models, Applications and Realizations", scientific reports, 15 July 2019.
[53] Smith, D.R., Padilla,W.J., Vier, D., Nemat-Nasser, S.C., and Schultz, S. "Composite medium with simultaneously negative permeability and permittivity", Physical Review Letters, 2000, 84, (18), pp. 4184.
[54] Dong, Y., Toyao, H., and Itoh, T.: 'Design and characterization of miniaturized patch antennas loaded with complementary split-ring resonators', IEEE Transactions on. Antennas and Propagations., 2012, 60, (2), pp. 772–785.
[55] Z. Mousavi Razi, P. Rezaei, "Fabry Perot Cavity Antenna Based on Capacitive Loaded Strips Superstrate for X-Band Satellite Communication", ARS JOURNAL, VOL. 2, NO. 1, DECEMBER 2013.
[56] Edward J. Rothwell, Jonathan L. Frasch, Sean M. Ellison, Premjeet Chahal, and Raoul O. Ouedraogo, "Analysis of the Nicolson-Ross-Weir Method for Characterizing the Electromagnetic Properties of Engineered Materials", Progress In Electromagnetics Research, Vol. 157, 31–47, 2016.
[57] Muhammad Hamza and Wasif T. Khan, "Hybrid Utilization of Loading Techniques and Cavity Groove for Performance Enhancement of the UWB (2–18GHz) Spiral Antenna", International Journal of Antennas and Propagation, Vol. 2018, 8 pages, 2018.
[58] Christian Ballesteros, Andreas Pfadler, Jordi Romeu, Lluis Jofre, "5G Vehicle MIMO Antenna Capacity Based on a Rigorous Electromagnetic Channel Modeling", 48th European Microwave Conference (EuMC), Sept. 2018.
[59] Syeda Fizzah Jilani, Qammer H. Abbasi, Akram Alomainy, "Inkjet-Printed Millimetre-Wave PET-Based Flexible Antenna for 5G Wireless Applications", 2018 IEEE MTT-S International Microwave Workshop Series on 5G Hardware and System Technologies (IMWS-5G), Aug 2018.
[60] Husameldin Abdelrahman Elmobarak Elobaid, Sharul Kamal Abdul Rahim, Mohamed Himdi, Xavier Castel, and Mohammad Abedian Kasgari, "A Transparent and Flexible Polymer-Fabric Tissue UWB Antenna for Future Wireless Networks", IEEE ANTENNAS AND WIRELESS PROPAGATION LETTERS, Vol. 16, 2017.
[61] Weiwei Li, Azat Meredov, and Atif Shamim, "Silver Nanowire based Flexible, Transparent, Wideband Antenna for 5G Band Application", 2019 IEEE International Symposium on Antennas and Propagation and USNC-URSI Radio Science Meeting, Oct 2019.
[62] Balaka Biswas, Rowdra Ghatak, and D. R. Poddar, "A Fern Fractal Leaf Inspired Wideband Antipodal Vivaldi Antenna for Microwave Imaging System", IEEE TRANSACTIONS ON ANTENNAS AND PROPAGATION, Vol. 65, no. 11, NOVEMBER 2017.
[63] Paul A.J. Kolarsick, Maria Ann Kolarsick, and Carolyn Goodwin, "Anatomy and Physiology of the Skin", 2006.
[64] https://www.healthline.com/health/stratum-corneum#function.
[65] Tale Saeidi, Idris Ismail, Adam R. H. Alhawari, and Wong Peng Wen, "Near-field and far-field investigation of miniaturized UWB antenna for imaging of wood", AIP advances, Vol. 9, 2019.
[66] Tale Saeidi, Idris Ismail, Sarmad Nozad Mahmood, Sameer Alani, and Adam R. H. Alhawar, "Microwave Imaging of Voids in Oil Palm Trunk Applying UWB Antenna and Robust Time-Reversal Algorithm", Journal of Sensors, Volume 2020, Article ID 8895737, 21 pages.
[67] H.-J. Li, T.-Y. Liu, and S.-H. Yang, "Superhigh image resolution for microwave imaging," International Journal of Imaging and Technology, vol. 2, no. 1, pp. 37–46, 1990.

[68] N. Simonov, S.-H. Son, B.-R. Kim, and S.-I. Jeon, "Investigation of spatial resolution in a microwave tomography system," in 2014 International Conference on Electronics, Information and Communications (ICEIC), pp. 305–700, Kota Kinabalu, Malaysia, January 2014.

[69] N. A. Simonov, S. I. Jeon, S. H. Son, J. M. Lee, and H. J. Kim, about equivalency of two methods of information gathering in microwave imaging, Radio Technology Research Department, ETRI, Daejeon, South Korea, 2012.